Skin integrated with perfusable vascular channels on a chip

Nobuhito Mori[1], Yuya Morimoto[1] and Shoji Takeuchi[1, 2*]

[1]Center for International Research on Integrative Biomedical Systems (CIBiS), Institute of Industrial Science (IIS), The University of Tokyo, 4-6-1 Komaba, Meguro-ku, Tokyo 153-8505, Japan

[2]Takeuchi Biohybrid Innovation Project, Exploratory Research for Advanced Technology (ERATO), Japan Science and Technology (JST), Komaba Open Laboratory (KOL) Room M202, 4-6-1, Komaba, Meguro-ku, Tokyo 153-8904, Japan

* e-mail: takeuchi@iis.u-tokyo.ac.jp; Tel.: +81-3-5452-6650; Fax: +81-3-5452-6649

Note:

This file is an accepted manuscript. See https://doi.org/10.1016/j.biomaterials.2016.11.031 to get published version.

Abstract

This paper describes a method for fabricating perfusable vascular channels coated with endothelial cells within a cultured skin-equivalent by fixing it to a culture device connected to an external pump and tubes. A histological analysis showed that vascular channels were constructed in the skin-equivalent, which showed a conventional dermal/epidermal morphology, and the endothelial cells formed tight junctions on the vascular channel wall. The barrier function of the skin-equivalent was also confirmed. Cell distribution analysis indicated that the vascular channels supplied nutrition to the skin-equivalent. Moreover, the feasibility of a skin-equivalent containing vascular channels as a model for studying vascular absorption was demonstrated by measuring test molecule permeation from the epidermal layer into the vascular channels. The results suggested that this skin-equivalent can be used for skin-on-a-chip applications including drug development, cosmetics testing, and studying skin biology.

1. Introduction

The skin is the largest human organ and functions as a barrier between the internal and external environments. The functions of skin include temperature regulation, tactile sensing, and the prevention of water loss in association with its vascular network, nerve system, and appendages (e.g. sweat glands, sebaceous glands, and hair follicles) [1–3].

To assist studies on the medical treatment of the skin, a skin model consisting of dermal and epidermal layers, known as a skin-equivalent, was developed in the 1980s [4]. The skin-equivalent model has been used not only as a tool in clinical dermatology and for wound coverage, but also as an alternative to animal experiments in the development of drugs and cosmetics [5]. In addition, studies have integrated skin-equivalents with various cells, structures, and appendages to mimic human skin [3,6–10]. In particular, the construction of vascular channels within a skin-equivalent has attracted considerable attention because a skin-equivalent with vascular channels could be used in applications including angiogenesis studies [11], graft survival improvement [12], angiostatic drug evaluation [13], and cancer research [14]. Moreover, the construction of vascular channels would be an important step towards implementing hair, sweat glands, nervous system, and immune system components because vascular channels can deliver nutrition to these features.

To construct vascular channels, skin-equivalents containing capillary networks have been developed by seeding stem cells or endothelial cells into the dermal layer and inducing vascularization. Such models have been used in studies of angiogenesis and skin grafting, and for drug testing [13,15–

17]. However, the vascular channels formed in those studies, which were composed of capillary networks, could not be perfused using an external pump because they were inaccessible owing to their spontaneous and random formation in the dermal layer. Consequently, supplying nutrients or sampling media via the vascular channels remains difficult, limiting the applicability of those models.

Here, we fabricated perfusable vascular channels in a skin-equivalent model (Fig. 1a). The vascular channels were coated with endothelial cells and supplied nutrition to the skin-equivalent. Both edges of the vascular channels were fixed to the connectors of a culture device attached to a perfusion system composed of a peristaltic pump and silicone tubes. We cultured the skin-equivalent under perfusion conditions and confirmed that it had dermal/epidermal layers and a barrier function. Moreover, we investigated the influence of medium perfusion on the skin-equivalent by analyzing the cell distribution following perfusion and non-perfusion. Finally, to demonstrate the potential applications of the skin-equivalent in dermatological studies and for drug testing, we applied test drugs to the epidermis and measured the amounts absorbed into the vascular channels.

2. Materials and methods

2.1. Reagents

Fibroblast growth medium (FGM)-2, endothelial growth medium (EGM)-2, and keratinocyte growth medium-Gold™ were purchased from Lonza, Ltd. (Basel, Switzerland). Dulbecco's modified Eagle's medium (DMEM), Ham's nutrient mixture F-12 (Ham's F-12), penicillin-streptomycin,

hydrocortisone, adenine, caffeine, isosorbide dinitrate (ISDN), rhodamine B, fluorescein isothiocyanate-dextran (FITC-dextran, 20 kDa), and rhodamine B isothiocyanate-dextran (RITC-dextran, 70 kDa) were purchased from Sigma-Aldrich (St. Louis, MO, USA). Fetal bovine serum was purchased from Biosera (Kansas City, MO, USA). Phosphate-buffered saline without Mg^{2+} and Ca^{2+} (PBS^{-}) was purchased from Cell Science & Technology Institute (Sendai, Japan). Type I collagen solution (IAC-50) was purchased from Koken Co. (Tokyo, Japan). L-ascorbic acid phosphate magnesium salt *n*-hydrate (ascorbic acid), insulin, vascular endothelial growth factor (VEGF), and acetonitrile were purchased from Wako Pure Chemical Industries (Osaka, Japan). Four percent paraformaldehyde solution (PFA) was purchased from Muto Pure Chemicals Co., Ltd. (Tokyo, Japan). Dimethyl sulfoxide was purchased from Kanto Chemical Co., Inc. (Tokyo, Japan). The topical skin adhesive DERMABOND ADVANCED® was purchased from Ethicon LLC (Somerville, NJ, USA). Type IV collagen antibody, cytokeratin 10 (CK10) antibody, and cytokeratin 15 (CK15) antibody were purchased from Abcam PLC (Cambridge, UK). CD31 antibody was purchased from BD Biosciences (San Jose, CA, USA). ZO-1 antibody was purchased from Invitrogen (Carlsbad, CA, USA).

2.2. Cell culture

Normal human dermal fibroblasts (NHDFs) and normal human epidermal keratinocytes (NHEKs) were purchased from Lonza. Human umbilical vein endothelial cells (HUVECs) were purchased from PromoCell GmbH (Heidelberg, Germany). NHDFs, NHEKs, and HUVECs were maintained in FGM-

2, keratinocyte growth medium-Gold™, and EGM-2, respectively, at 37 °C under a 5% CO_2 atmosphere.

2.3. Fabrication of the culture device and skin-equivalent

The culture device was composed of a main part and a bottom plate fabricated using a 3D printer (AGILISTA-3100, KEYENCE Corp., Osaka, Japan) (Fig. 1b-1). Anchoring structures on the connectors kept the skin-equivalent fixed to the device. The main part and the bottom plate were assembled and coated with parylene C (2–4 μm thick) to increase biocompatibility and seal the gap (Fig. 1b-2). Then, nylon wires (0.52 mm diameter) were strung across the connectors of the device. The device and nylon wires were sterilized using 70% ethanol and ultraviolet irradiation. Next, the parylene layer of the device was treated with O_2 plasma using a plasma etcher (FA-1, Samco, Inc., Kyoto, Japan) to increase cell and collagen gel adhesion onto the device. Within 1 h after O_2 plasma treatment, the device was filled with neutralized collagen solution composed of IAC-50, 10× PBS^-, and FGM-2 containing 8×10^5 cells/mL of NHDFs and incubated at 37 °C for 30–60 min until the collagen gel formed a dermis-like layer (Fig. 1b-3). The ratio of IAC-50, 10× PBS^-, and FGM-2 containing NHDFs was 9:1:17 in the experiment evaluating the effectiveness of using anchoring structures and O_2 plasma treatment to keep the skin-equivalent fixed to the device, and 9:1:5 in other experiments. The nylon wires were strung in a grid pattern to evaluate the effectiveness of anchoring structures and O_2 plasma treatment, while they were straight in other experiments. The dermal layer

was removed from the side walls of the device using a pipette tip and incubated in DMEM containing 10% fetal bovine serum, 1% penicillin-streptomycin, and 70 μg/mL ascorbic acid for 2–3 days to induce shrinkage. After shrinkage of the dermal layer, the medium was changed to EGM-2 (Fig. 1b-4). Hollow channels were made by removing the nylon wires. Each hollow channel was filled with 200 μL of EGM-2 containing 4×10^5 HUVECs using a syringe pump (KD Scientific, Holliston, MA, USA). After 20 min of incubation, the device was inverted to coat the upper half of the channels with HUVECs. After another 20 min of incubation, the device was inverted again and incubated for 2 days to form the vascular channels. Subsequently, the medium was changed to FAD culture medium (DMEM and Ham's F-12 [3:1] supplemented with 10% fetal bovine serum, 1% penicillin-streptomycin, 70 μg/mL ascorbic acid, 0.4 μg/mL hydrocortisone, 5 μg/mL insulin, and 25 μg/mL adenine) to form the epidermal layer (Fig. 1b-5). Next, 550 μL of FAD containing 1.1×10^6 NHEKs was poured into a square-shaped silicone rubber barrier enclosing a surface area of 1.44 cm^2 and placed on the dermal layer. After 1 day of incubation and removal of the rubber barrier, the skin-equivalent (i.e., a dermal layer seeded with NHEKs) was lifted to the air-liquid interface to induce cornification of the epidermal layer. Perfusion of FAD was simultaneously conducted using a peristaltic pump (SJ-1211II-L, ATTO Corp., Tokyo, Japan, or MINIPULS® 3, Gilson Inc., Middleton, WI, USA) at 2–3 mL/h (Fig. 1c). Half of the medium was changed every 2 or 3 days.

2.4. Histological analysis

To analyze the morphology of the skin-equivalent and vascular channels, the samples were subjected

to hematoxylin and eosin (HE) staining and immunostaining. For HE staining, after 10 days of perfusion culture, the samples were fixed in PFA, cryosectioned, and stained with Mayer's hematoxylin and 0.5% eosin Y ethanol solution. The HE-stained sections were observed using bright field microscopy (IX71, Olympus Corp., Tokyo, Japan).

For the immunostaining of type IV collagen, CK10, and CK15, the samples were also fixed in PFA and cryosectioned after 10 days of perfusion culture. The sections were washed with PBS^- and blocked with 1% bovine serum albumin (BSA). Subsequently, the primary antibody solution diluted 1:200 in 1% BSA was applied and incubated for at least 8 h at 4 °C. The sections were washed with PBS^- and incubated with secondary antibody solution diluted 1:200 in 1% BSA for 2 h at room temperature. The sections were counterstained with 4′,6-diamidino-2-phenylindole (DAPI). For the immunostaining of CD31, the samples were snap-frozen without fixation and cryosectioned. The sections were washed with PBS^- and blocked with 1% BSA. Subsequently, the primary antibody solution diluted 1:200 in 1% BSA was applied and incubated for at least 2 h at room temperature. The sections were washed with PBS^- and incubated with a secondary antibody solution diluted 1:200 in 1% BSA for 1 h at room temperature. The sections were fixed in PFA and counterstained with DAPI. The immunostained sections were observed by confocal microscopy (LSM 7 DUO, Carl Zeiss, Oberkochen, Germany).

For the immunostaining of ZO-1, after 6 days of perfusion culture, the samples were fixed in PFA for 3–4 h. Next, the samples were washed with PBS^- and the vascular channels were filled with

0.1% Triton™ X-100 in 1% BSA using a syringe pump. After 20 min of incubation, the vascular channels were washed with 1% BSA and incubated for 1 h at room temperature. The vascular channels were filled with primary antibody solution diluted 1:100 in 1% BSA and incubated for 8 h at 4 °C. The primary antibody solution was washed out with 1% BSA. The vascular channels were filled with secondary antibody solution diluted 1:100 in 1% BSA and incubated for at least 2 h at room temperature. The immunostained vascular channels were observed using two-photon excitation microscopy (LSM780 NLO, Carl Zeiss).

2.5. Functional analysis

To evaluate the barrier function of the epidermal layer, we added 100 μL of PBS^- to the epidermis of the skin-equivalent and observed whether the liquid was repelled and formed droplets. Moreover, using an LCR meter (LCR700, Sanwa Electric Instrument Co., Ltd., Tokyo, Japan), we measured the capacitance of the epidermal layer to assess the performance of its barrier function [18,19]. The measurement was performed at 1 kHz by placing electrodes 5 mm apart on the surface of the epidermal layer. We also measured the capacitance of the dermal layer by placing electrodes on the surface near the edge of the skin-equivalent where the epidermal layer was not formed and the dermal layer was exposed to air. The unpaired Student's *t*-test was used to compare the data.

To evaluate the function of the vascular channels as a nutrition supply pathway, we measured the cell distribution in the skin-equivalent after 10 days of perfusion culture. Images of the sections stained with DAPI were acquired by fluorescent microscopy (IX71, Olympus Corp.). The number of

cells was measured for each 100-μm interval from the upper and lower edges of the vascular channels using ImageJ software (NIH, Bethesda, MD, USA) (Fig. S1). To achieve this, the images were converted to binary by threshold and watershed processes, and particles larger than 79 μm^2, which is equivalent to the area of a 10-μm diameter circle, were counted as cells in the sections using the 'analyze particles' function of ImageJ. The epidermal layer was excluded from this analysis. The cell density of each region was calculated using the thickness value of 7 μm for the section.

2.6. Measurement of percutaneous absorption

To demonstrate the feasibility of using the skin-equivalent for drug development, we measured the percutaneous absorption of caffeine and ISDN as model drugs. We prepared two groups for the measurement: a group stimulated with 20 ng/mL of VEGF and a group not stimulated with VEGF. The addition of VEGF to FAD was performed 2 days before the measurement. On the day of measurement, we adhered a reservoir composed of silicone (8 mm in diameter and 0.5 mm in thickness) to the epidermal layer using DERMABOND ADVANCED®. The skin-equivalent was placed on DMEM in the chamber and infused with DMEM at a flow rate of 6 mL/h. We collected the drained DMEM from the channel at 15, 30, 45, 60, and 75 min after starting infusion. We also collected DMEM under the skin-equivalent and added the same amount of new DMEM. Next, 100 μL of caffeine and ISDN solution was added to the reservoir immediately after the first sampling at 15 min. The caffeine and ISDN solution was prepared by mixing 20 mg/mL caffeine in PBS^- and 100 mg/mL ISDN in dimethyl sulfoxide at a ratio of 10:1. The samples were analyzed using HPLC (ACQUITY UPLC H-Class,

Waters Corp., Milford, MA, USA). Caffeine was detected at 220 nm in the mobile phase composed of water and acetonitrile (90:10) at a flow rate of 0.6 mL/min. ISDN was detected at 220 nm in the mobile phase composed of water and acetonitrile (50:50) at a flow rate of 0.6 mL/min. An external standard method was used for quantitative analysis. The unpaired Student's *t*-test was performed to compare the data at each time point. The lag time was estimated by fitting lines to the data points at 45, 60, and 75 min for samples from under the skin-equivalent and 30, 45, and 60 min for samples from the vascular channels.

3. Results and discussion

3.1. Evaluation of anchoring structure and O_2 plasma treatment

To demonstrate the effectiveness of the anchoring structures for keeping the skin-equivalent attached to the culture device for creating perfusable channels, we compared culture devices with and without anchoring structures. We found that the dermal layer was detached from the culture device without anchoring structures when the nylon wires were removed (Fig. 2a), while the dermal layer remained attached to the culture device when the anchoring structures were present (Fig. 2b). This result indicates that the anchoring structures effectively held the dermal layer in place.

We also investigated the influence of O_2 plasma treatment on the attachment of tissue to the culture device. The skin-equivalent was detached from the device without O_2 plasma treatment during perfusion culture (Fig. 2c), whereas the skin-equivalent remained attached to the device with O_2 plasma treatment (Fig. 2d). We cultured the skin-equivalents under perfused condition up to 2 weeks;

some experimental replicates failed to perfuse due to the channel clogging after approximately 1 week of perfusion culture. The duration of perfusion (1–2 weeks) is enough for the permeation test performed in this paper, while the investigation of the clogging mechanism and the extension of the perfusion duration are challenges that will need to be considered in future work. When we infused blue ink into the device without O_2 plasma treatment, the infused ink did not drain from the outlet, but leaked from the gap between the dermal layer and device, whereas the ink drained from the outlet of the device treated with O_2 plasma (Fig. 2e). Therefore, O_2 plasma treatment probably increased the adhesiveness of NHDFs and collagen on parylene as previously reported [20–22]. These results indicate that using the anchoring structures and O_2 plasma treatment in combination is effective for maintaining the perfusability of the skin-equivalent by firmly fixing it to the culture device.

3.2. Histological analysis

To analyze the morphology of the fabricated skin-equivalent, we evaluated the cryosections of perfused and non-perfused samples by HE staining and immunostaining. As shown in Fig. 3a and b, the skin-equivalent exhibited epidermal/dermal layers and vascular channels. The HE-stained sections revealed that an epidermal layer was formed in both perfused and non-perfused samples (Fig. 3c and d). The epidermal thickness of the perfused skin-equivalent was approximately 50 μm, which was comparable to that of a skin-equivalent fabricated by the conventional method (approximately 50 μm) [23] and a skin-equivalent sold on the market (28–43 μm; EpiDerm™, MatTek Corp., Ashland, MA, USA) [24]. In addition, CK15 and CK10 were localized to the basal layer and the upper layer (Fig. 3e and f),

respectively, indicating that normal differentiation was induced in the epidermal layers of both the perfused and non-perfused skin-equivalents [24,25].

The perfusion condition influenced the morphology of the vascular channels. While there was no significant influence of the perfusion condition on the epidermal layer, the vascular channels were open in the perfused skin-equivalent, whereas they were nearly closed in the non-perfused condition (Fig. 3g and h). This influence was quantitatively evaluated by measuring the cross-sectional area of the vascular channels in the perfused and non-perfused skin-equivalents. The cross-sectional area of the perfused skin-equivalent was approximately 6-fold larger than that of the non-perfused one (Fig. S2). These results indicated that the vascular channels were open because of the pressure generated by perfusion. Immunostaining revealed the presence of a basement membrane protein (type IV collagen) and a marker of HUVECs (CD31) on the channel surface (Fig. 3i–l). We also observed the vascular channels before perfusion by immunostaining them for CD31 and using two-photon excitation microscopy. The results confirmed that the channels were coated by HUVECs (Fig. S3). Moreover, confocal images showed that ZO-1 coated the wall of the vascular channels (Fig. 3m), indicating that the HUVECs formed tight junctions within the channels. These results indicated that our skin-equivalent had perfusable vascular channels with tight junction formation in addition to a conventional epidermal and dermal morphology.

3.3. Functional analysis

To demonstrate the barrier function of the epidermal layer, we investigated the water repellency and

capacitance of the epidermal layer on the perfused skin-equivalent. When 100 μL of PBS^{-} was applied to the epidermis, it was repelled and formed a droplet (Fig. 3n). Typically, such PBS^{-} droplets were not absorbed but maintained their shape on the epidermal layer for more than 1 h, while water generally spread and became absorbed into the dermal layer. Additionally, the capacitance of the epidermal layer was significantly lower than that of the dermal layer (Fig. 3o). The capacitance further decreased with an increasing concentration of NHEKs, eventually resulting in a value comparable to that of the skin-equivalent fabricated by the conventional method [23] (Fig. S4). These results indicated that the barrier function of the epidermal layer was well organized even under the perfusion condition and could be controlled by changing the concentration of NHEKs.

Next, to evaluate material diffusion from the vascular channels, we infused 3 types of fluorescent dye molecules into the vascular channels: rhodamine B (479 Da), FITC-dextran (20 kDa), and RITC-dextran (70 kDa). We studied the vascular channels in the dermal layer without seeding NHEKs and performed the experiment after 4 or 5 days of perfusion culture. Fluorescent images were acquired by fluorescent microscopy (IX71, Olympus Corp.). The results showed that an increase in fluorescent intensity was detected on the outside of the channels for each fluorescent dye, indicating the diffusion of the fluorescent molecules (Fig. S5a-c). We also calculated the permeability of the fluorescent molecules by analyzing the acquired images using a previously reported method [26]. The permeability showed an inverse relationship with molecular weight and was on the same order as that previously reported for a 70-kDa molecule [27] (Fig. S5d). These findings indicated that a size-

selective barrier was formed by the HUVECs lining the vascular channels.

To examine the biological effects of the nutrient supply from the vascular channels to the skin-equivalent, we measured the cell distributions of the perfused and non-perfused skin-equivalents (Fig. 4). The average cell density of the perfused skin-equivalent (6×10^7 cells/mL) was higher than that of the non-perfused skin-equivalent (2×10^7 cells/mL). The ratio of the upper and lower thicknesses differed between the perfused and non-perfused skin-equivalents, although the total thickness was the same in each condition. It is assumed that this difference was caused by the fabrication error of the nylon wire stringing. Regarding the cell distribution, the cell densities of both the perfused and non-perfused skin-equivalents were high around the vascular channels and decreased with an increasing distance from the channels. The cell density was highest in the depth range of 0–100 μm of the perfused skin-equivalent, which was approximately 4-fold higher than that in the same depth range of the non-perfused skin-equivalent. These results indicated that nutrition and oxygen were supplied to the cells from the vascular channels. Therefore, our perfusion system would be useful for fabricating thick and dense tissues. The cell density around the vascular channels was maintained on the order of 10^8 cells/mL, which is generally difficult to achieve in the deep part of the tissue because of diffusion limitations [28].

3.4. Measurement of percutaneous absorption

To investigate the influence of vascular perfusion on percutaneous absorption, we monitored the permeation of test molecules, caffeine and ISDN, through the skin-equivalent during the perfusion of

DMEM in the vascular channels (Fig. 5a and b). In the experiment, we measured the concentrations of permeated caffeine and ISDN in media collected either from beneath the skin-equivalent [medium A, designated by (A) in Fig. 5] or from the vascular channels [medium B, designated by (B) in Fig. 5]. As a result, permeated molecules were detected in both medium A and B as shown in Fig. 5c–f. The total number of permeated molecules, which was calculated from the measured concentration, was normalized to the initial amount of molecules applied to the skin-equivalent (9.4 μmol of caffeine and 3.8 μmol of ISDN). The lag times of caffeine and ISDN, which were defined as the elapsed times from x = 15 min (i.e., the application time of the test molecules) to the x-intercepts of the dotted lines, were smaller in medium B (~ 5 min) than in medium A (~ 30 min). This result can be explained based on the morphology of the skin-equivalent and indicates that caffeine and ISDN first reached the vascular channel and then the bottom of the skin-equivalent. Moreover, the normalized permeated amount of ISDN was 3–4-fold higher than that of caffeine, indicating differences in permeability between caffeine and ISDN; these results are consistent with those of a previous report examining human skin and a conventional skin model [29].

To confirm whether the vascular channels showed endothelial functions, we measured the permeation of the test molecules in the presence and absence of VEGF ($VEGF^+$ and $VEGF^-$, respectively). In medium A, caffeine and ISDN permeation in the $VEGF^+$ condition was lower or did not significantly differ compared to their permeation in the $VEGF^-$ condition (Fig. 5c and d). In contrast, in medium B, permeation in the $VEGF^+$ condition was significantly higher than that in the

VEGF^{-} condition after 45 min (Fig. 5e and f). These results indicated that vascular channel permeability is controlled by VEGF. Moreover, our skin-equivalent integrated with vascular channels can be used as a model of vascular absorption because the vascular channels showed an endothelial function (the increase of vascular permeability by VEGF) similar to that *in vivo* [30].

4. Conclusion

We developed a skin-equivalent integrated with perfusable vascular channels. Because of the presence of anchoring structures and the O_2 plasma treatment of parylene, the skin-equivalent was stably fixed to the device and was perfusable during the cultivation period. The vascular channels served as a nutrition delivery pathway; the cell density of the perfused skin-equivalent was higher than that of the non-perfused skin-equivalent. Moreover, the vascular channels in the skin-equivalent showed feasibility as a model of vascular absorption. Therefore, our skin-equivalent is useful for skin-on-a-chip applications including drug development, cosmetics testing, and the reconstruction of skin appendages.

Acknowledgments

N. Mori was supported by a Grant-in-Aid for fellows from the Japan Society for the Promotion of Science (JSPS) (no. 26-7064). Y. Morimoto was supported by the Mazda Foundation and a Grant-in-Aid for Challenging Exploratory Research from the JSPS (no. 15K13904). We greatly appreciate

Sacha Salameh for fruitful discussions.

References

[1] M. Van Gele, B. Geusens, L. Brochez, R. Speeckaert, J. Lambert, Three-dimensional skin models as tools for transdermal drug delivery: challenges and limitations, Expert Opin. Drug Deliv. 8 (2011) 705–720. doi:10.1517/17425247.2011.568937.

[2] E.A. Lumpkin, M.J. Caterina, Mechanisms of sensory transduction in the skin, Nature. 445 (2007) 858–865. doi:10.1038/nature05662.

[3] S. Huang, Y. Xu, C. Wu, D. Sha, X. Fu, In vitro constitution and in vivo implantation of engineered skin constructs with sweat glands, Biomaterials. 31 (2010) 5520–5525. doi:10.1016/j.biomaterials.2010.03.060.

[4] E. Bell, H. Ehrlich, D. Buttle, T. Nakatsuji, Living tissue formed in vitro and accepted as skin-equivalent tissue of full thickness, Science. 211 (1981) 1052–1054. doi:10.1126/science.7008197.

[5] F. Groeber, M. Holeiter, M. Hampel, S. Hinderer, K. Schenke-Layland, Skin tissue engineering — In vivo and in vitro applications, Adv. Drug Deliv. Rev. 63 (2011) 352–366. doi:10.1016/j.addr.2011.01.005.

[6] G. Lammers, G. Roth, M. Heck, R. Zengerle, G.S. Tjabringa, E.M. Versteeg, T. Hafmans, R. Wismans, D.P. Reinhardt, E.T.P. Verwiel, P.L.J.M. Zeeuwen, J. Schalkwijk, R. Brock, W.F. Daamen, T.H. van Kuppevelt, Construction of a microstructured collagen membrane mimicking the papillary dermis architecture and guiding keratinocyte morphology and gene

expression, Macromol. Biosci. 12 (2012) 675–691. doi:10.1002/mabi.201100443.

[7] M. Michel, N. L'Heureux, R. Pouliot, W. Xu, F.A. Auger, L. Germain, Characterization of a new tissue-engineered human skin equivalent with hair, Vitr. Cell. Dev. Biol. - Anim. 35 (1999) 318–326. doi:10.1007/s11626-999-0081-x.

[8] V. Facy, V. Flouret, M. Régnier, R. Schmidt, Langerhans cells integrated into human reconstructed epidermis respond to known sensitizers and ultraviolet exposure, J. Invest. Dermatol. 122 (2004) 552–553. doi:10.1046/j.0022-202X.2004.22209.x.

[9] A.L. Clement, T.J. Moutinho, G.D. Pins, Micropatterned dermal–epidermal regeneration matrices create functional niches that enhance epidermal morphogenesis, Acta Biomater. 9 (2013) 9474–9484. doi:10.1016/j.actbio.2013.08.017.

[10] N. Mori, Y. Morimoto, S. Takeuchi, Vessel-like channels supported by poly-l-lysine tubes, J. Biosci. Bioeng. (available online, 2016). doi:10.1016/j.jbiosc.2016.05.011.

[11] V. Hudon, F. Berthod, A.F. Black, O. Damour, L. Germain, F.A. Auger, A tissue-engineered endothelialized dermis to study the modulation of angiogenic and angiostatic molecules on capillary-like tube formation in vitro, Br. J. Dermatol. 148 (2003) 1094–1104. doi:10.1046/j.1365-2133.2003.05298.x.

[12] B. Hendrickx, J.J. Vranckx, A. Luttun, Cell-based vascularization strategies for skin tissue engineering., Tissue Eng. Part B. Rev. 17 (2011) 13–24. doi:10.1089/ten.TEB.2010.0315.

[13] P.-L. Tremblay, F. Berthod, L. Germain, F.A. Auger, In vitro evaluation of the angiostatic

potential of drugs using an endothelialized tissue-engineered connective tissue, J. Pharmacol. Exp. Ther. 315 (2005) 510–516. doi:10.1124/jpet.105.089524.

[14] T.R. Samatov, M.U. Shkurnikov, S.A. Tonevitskaya, A.G. Tonevitsky, Modelling the metastatic cascade by in vitro microfluidic platforms, Prog. Histochem. Cytochem. 49 (2015) 21–29. doi:10.1016/j.proghi.2015.01.001.

[15] A.F. Black, F. Berthod, N. L'heureux, L. Germain, F.A. Auger, In vitro reconstruction of a human capillary-like network in a tissue-engineered skin equivalent, FASEB J. 12 (1998) 1331–1340.

[16] A.S. Klar, S. Güven, T. Biedermann, J. Luginbühl, S. Böttcher-Haberzeth, C. Meuli-Simmen, M. Meuli, I. Martin, A. Scherberich, E. Reichmann, Tissue-engineered dermo-epidermal skin grafts prevascularized with adipose-derived cells, Biomaterials. 35 (2014) 5065–5078. doi:10.1016/j.biomaterials.2014.02.049.

[17] D. Marino, J. Luginbuhl, S. Scola, M. Meuli, E. Reichmann, Bioengineering dermo-epidermal skin grafts with blood and lymphatic capillaries, Sci. Transl. Med. 6 (2014) 221ra14. doi:10.1126/scitranslmed.3006894.

[18] J.C. Lawler, M.J. Davis, E.C. Griffith, Electrical characteristics of the skin: the impedance of the surface sheath and deep tissues, J. Invest. Dermatol. 34 (1960) 301–308. doi:10.1038/jid.1960.52.

[19] M.J. Goretsky, A.P. Supp, D.G. Greenhalgh, G.D. Warden, S.T. Boyce, Surface electrical

capacitance as an index of epidermal barrier properties of composite skin substitutes and skin autografts., Wound Repair Regen. 3 (1995) 419–425. doi:10.1046/j.1524-475X.1995.30406.x.

[20] T.Y. Chang, V.G. Yadav, S. De Leo, A. Mohedas, B. Rajalingam, C.L. Chen, S. Selvarasah, M.R. Dokmeci, A. Khademhosseini, Cell and protein compatibility of parylene-C surfaces, Langmuir. 23 (2007) 11718–11725. doi:10.1021/la7017049.

[21] T. Hoshino, I. Saito, R. Kometani, K. Samejima, S. Matsui, T. Suzuki, K. Mabuchi, Y.X. Kato, Improvement of neuronal cell adhesiveness on parylene with oxygen plasma treatment, J. Biosci. Bioeng. 113 (2012) 395–398. doi:10.1016/j.jbiosc.2011.11.003.

[22] T. Trantidou, C. Rao, H. Barrett, P. Camelliti, K. Pinto, M.H. Yacoub, T. Athanasiou, C. Toumazou, C.M. Terracciano, T. Prodromakis, Selective hydrophilic modification of Parylene C films: a new approach to cell micro-patterning for synthetic biology applications., Biofabrication. 6 (2014) 25004. doi:10.1088/1758-5082/6/2/025004.

[23] S. Amano, N. Akutsu, Y. Matsunaga, T. Nishiyama, M.F. Champliaud, R.E. Burgeson, E. Adachi, Importance of balance between extracellular matrix synthesis and degradation in basement membrane formation., Exp. Cell Res. 271 (2001) 249–262. doi:10.1006/excr.2001.5387.

[24] F. Netzlaff, C.-M. Lehr, P.W. Wertz, U.F. Schaefer, The human epidermis models EpiSkin®, SkinEthic® and EpiDerm®: An evaluation of morphology and their suitability for testing phototoxicity, irritancy, corrosivity, and substance transport, Eur. J. Pharm. Biopharm. 60

(2005) 167–178. doi:10.1016/j.ejpb.2005.03.004.

[25] B. Ataç, I. Wagner, R. Horland, R. Lauster, U. Marx, A.G. Tonevitsky, R.P. Azar, G. Lindner, Skin and hair on-a-chip: in vitro skin models versus ex vivo tissue maintenance with dynamic perfusion, Lab Chip. 13 (2013) 3555. doi:10.1039/c3lc50227a.

[26] G.M. Price, J. Tien, Methods for forming human microvascular tubes in vitro and measuring their macromolecular permeability, Methods Mol. Biol., 2011: pp. 281–293. doi:10.1007/978-1-59745-551-0_17.

[27] D.B. Kolesky, R.L. Truby, A.S. Gladman, T.A. Busbee, K.A. Homan, J.A. Lewis, 3D bioprinting of vascularized, heterogeneous cell-laden tissue constructs, Adv. Mater. 26 (2014) 3124–3130. doi:10.1002/adma.201305506.

[28] M. Radisic, J. Malda, E. Epping, W. Geng, R. Langer, G. Vunjak-Novakovic, Oxygen gradients correlate with cell density and cell viability in engineered cardiac tissue., Biotechnol. Bioeng. 93 (2006) 332–343. doi:10.1002/bit.20722.

[29] Kano Satoshi, Todo Hiroaki, Sugie Kenichi, Fujimoto Hidenori, Nakada Keiichi, Tokudome Yoshihiro, Hashimoto Fumie, Sugibayashi Kenji, Utilization of reconstructed cultured human skin models as an alternative skin for permeation studies of chemical compounds, Altern. to Anim. Test. Exp. 15 (2010) 61–70. doi:10.11232/aatex.15.61.

[30] W.G. Roberts, G.E. Palade, Increased microvascular permeability and endothelial fenestration induced by vascular endothelial growth factor., J. Cell Sci. 108 (1995) 2369–2379.

Figures

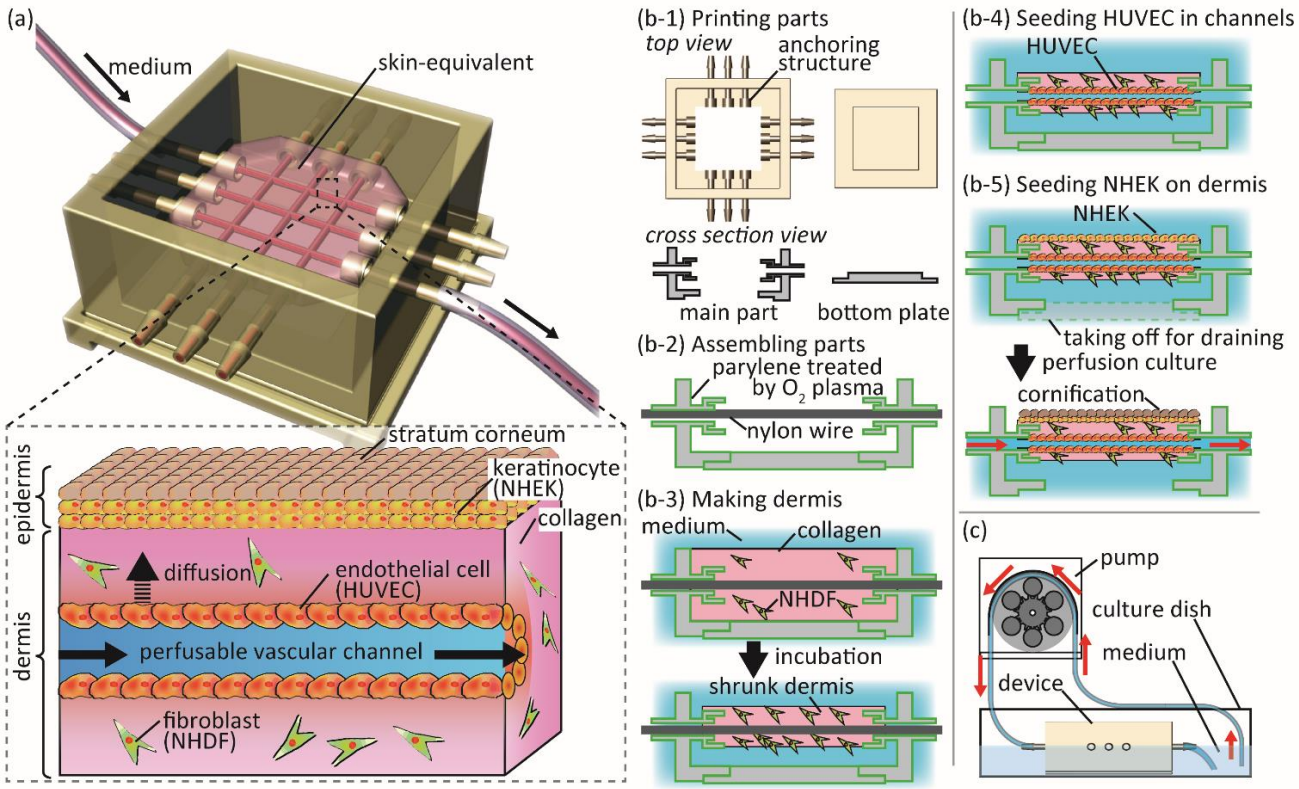

Figure 1. Schematic of skin-equivalent integrated with perfusable vascular channels and the fabrication process. (a) Conceptual illustration of the skin-equivalent and culture device. (b) Fabrication of the culture device and skin-equivalent. (c) Perfusion system composed of a peristaltic pump, silicone tubes, and a culture device.

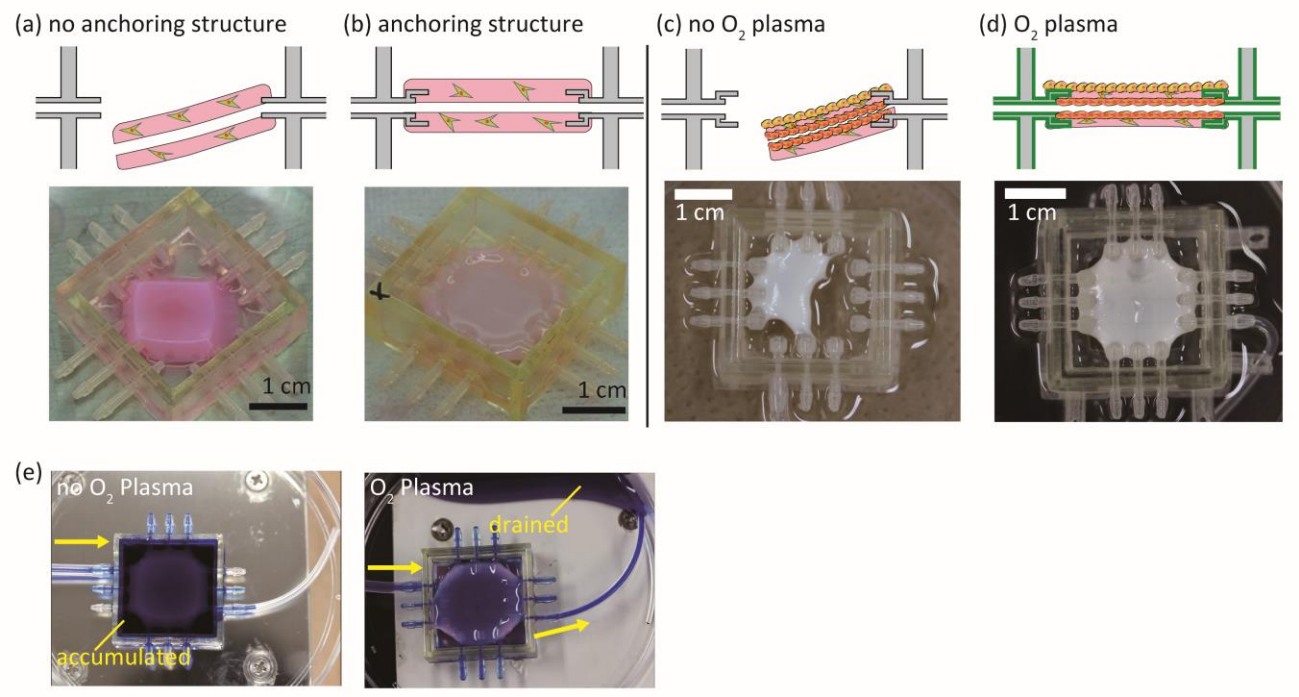

Figure 2. Evaluation of anchoring structures and O_2 plasma treatment. (a, b) Dermal layers cultured in the device without and with anchoring structures. (c, d) Skin-equivalents cultured in the device without and with O_2 plasma treatment. (e) Infusion of blue ink into the device without and with O_2 plasma treatment.

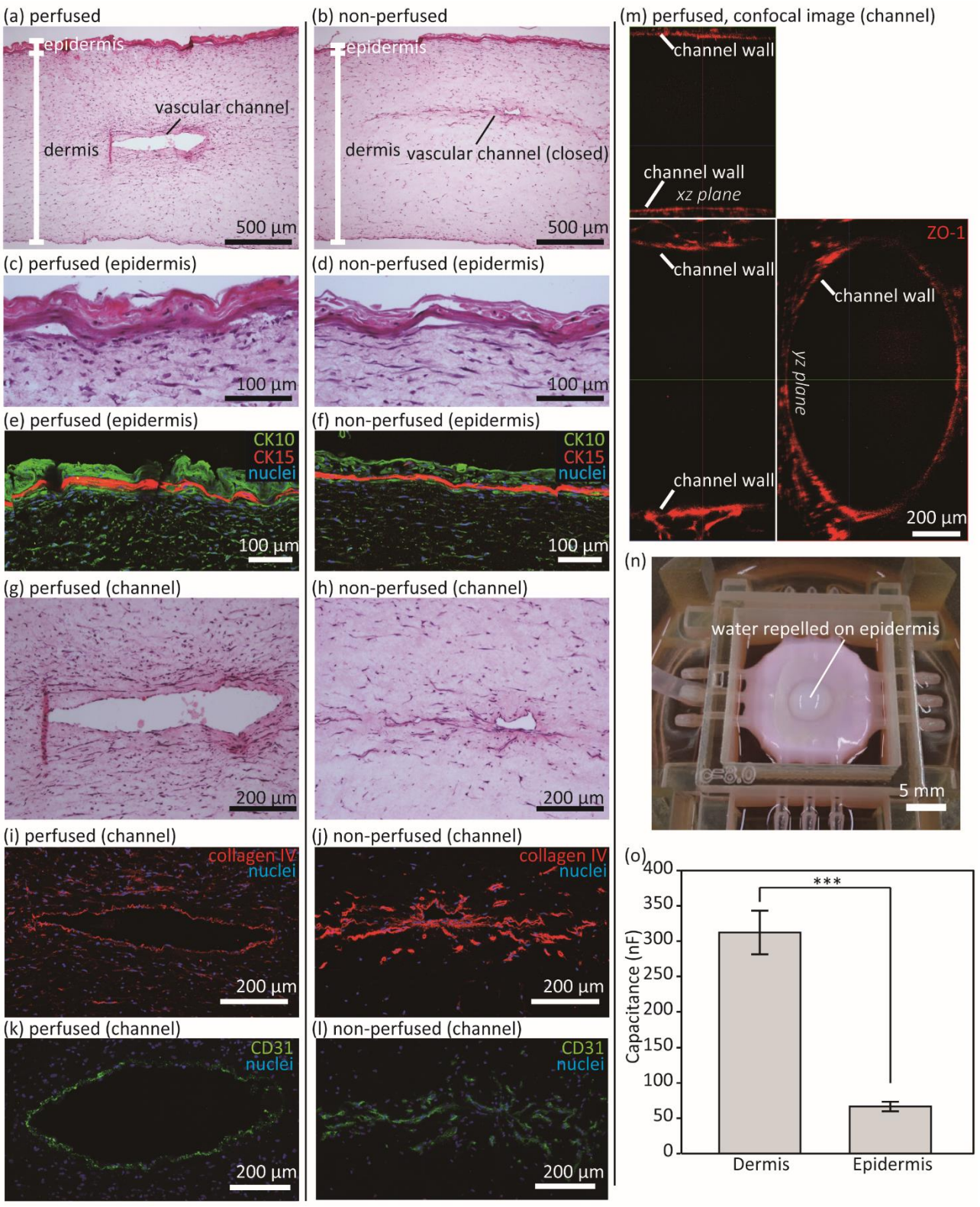

Figure 3. Histological analysis and barrier function assessment. (a, b) Hematoxylin and eosin (HE)-stained sections of perfused and non-perfused skin-equivalents. (c–f) Magnified images of the HE-stained and immunostained epidermal layers. (g–l) Magnified images of HE-stained and

immunostained vascular channels. (m) Confocal image of the vascular channel immunostained with ZO-1 antibody (stitched by ImageJ). (n) Barrier function evaluation by observing the repellency of water by the epidermal layer. (o) Barrier function assessment by capacitance measurement. The results are shown as the mean ± standard deviation (s.d.) of three devices. ***$p < 0.001$, unpaired Student's *t*-test.

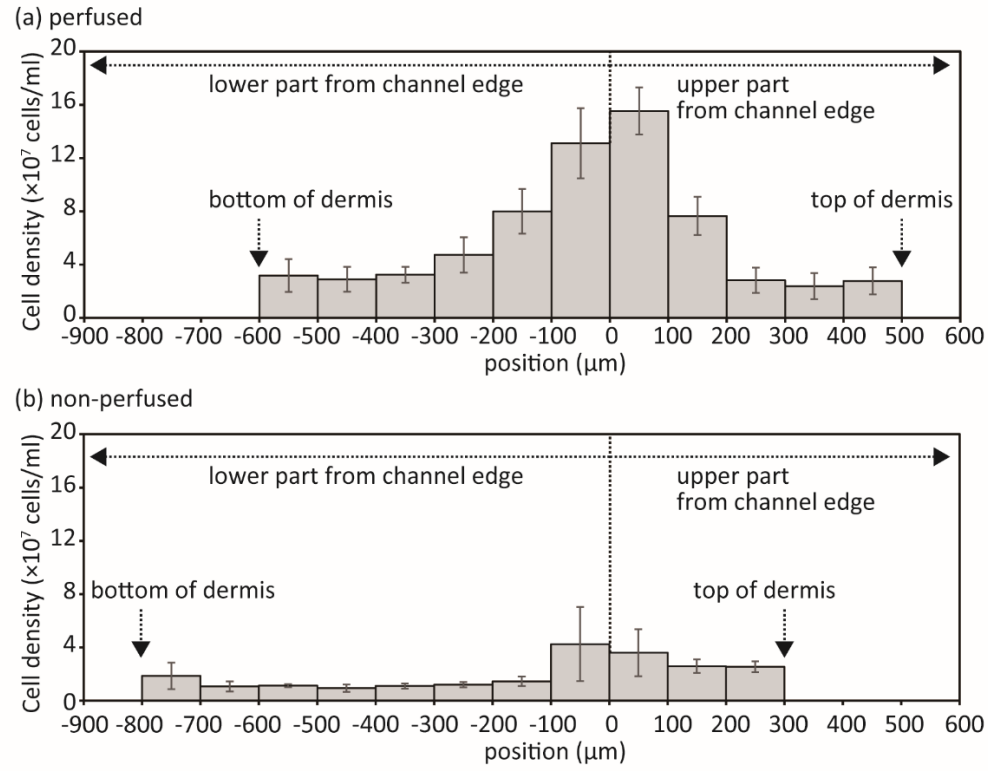

Figure 4. Cell distributions of the skin-equivalent cultured under perfused and non-perfused conditions. The results are shown as the mean ± s.d. of five sections from the same sample.

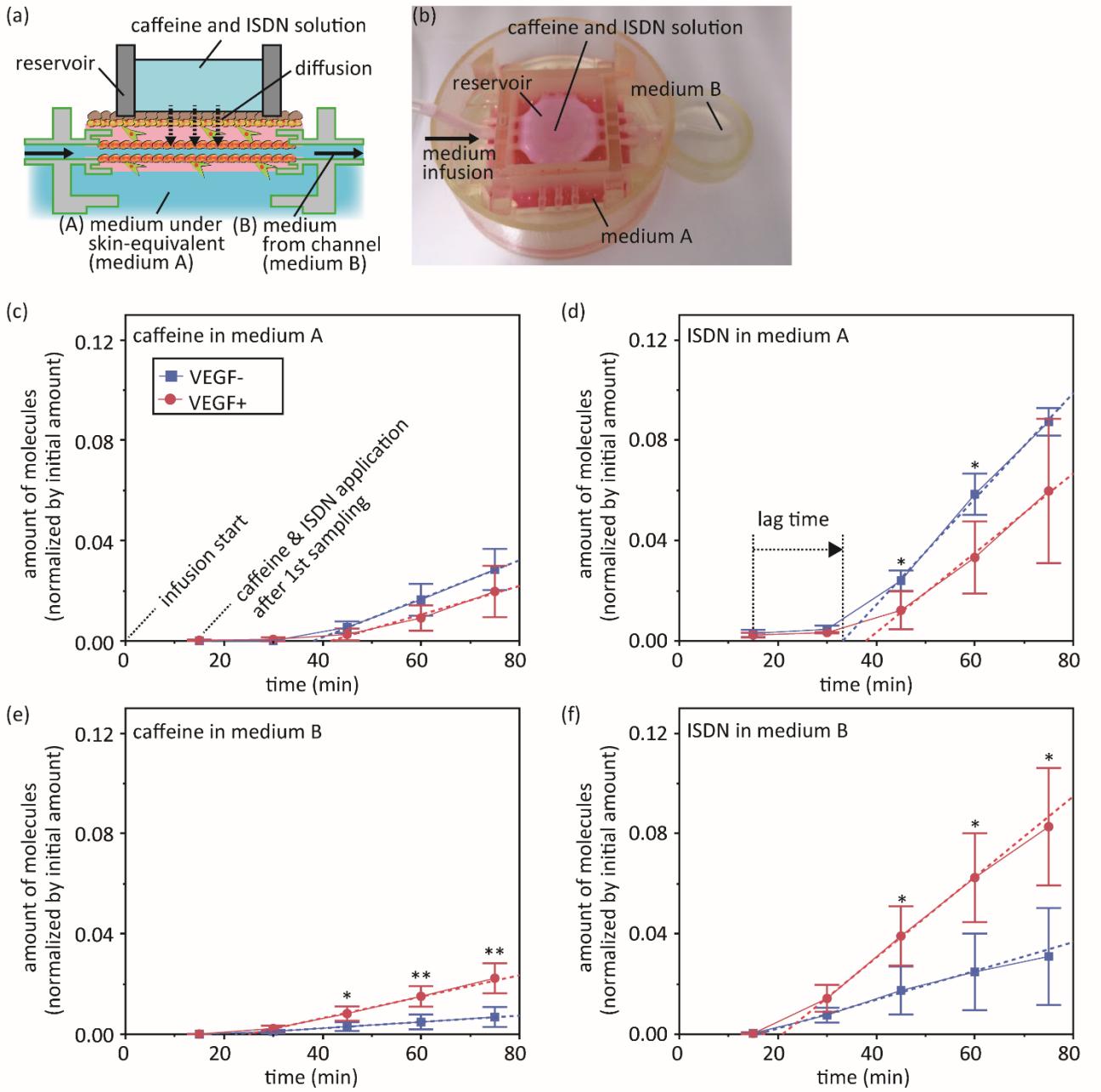

Figure 5. Percutaneous absorption measurement. (a, b) Schematic and photograph of the experimental setup. (c, d) Amounts of caffeine and ISDN permeating the medium beneath the skin-equivalents (medium A), normalized by the initial amounts of test molecules applied on the skin-equivalents. (e, f) Amounts of caffeine and ISDN permeating the medium taken from the vascular channels (medium B), normalized by the initial amounts of test molecules applied on the skin-equivalents. The results are shown as the mean ± s.d. of four devices. *$p < 0.05$, **$p < 0.01$, unpaired Student's t-test of the

difference between $VEGF^{-}$ and $VEGF^{+}$ at each time point.

SUPPLEMENTARY INFORMATION

Figures

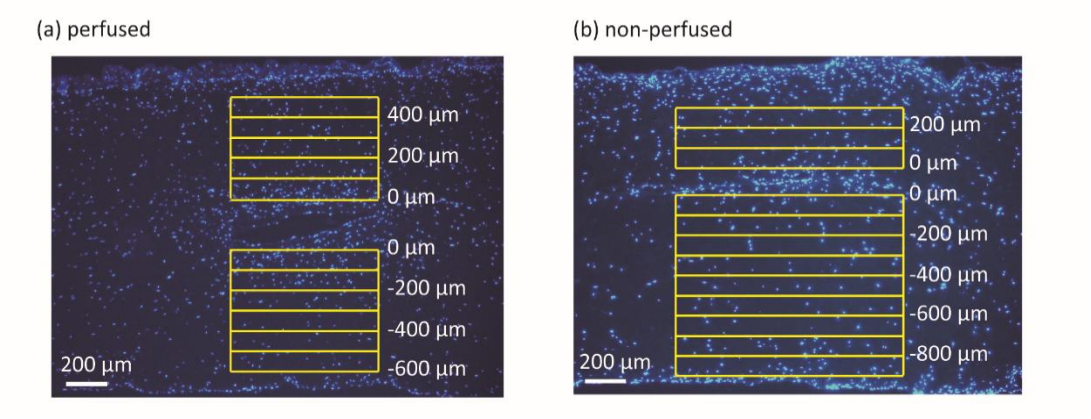

Figure S1. Measurement of cell distribution. The cell density within each yellow rectangle was measured.

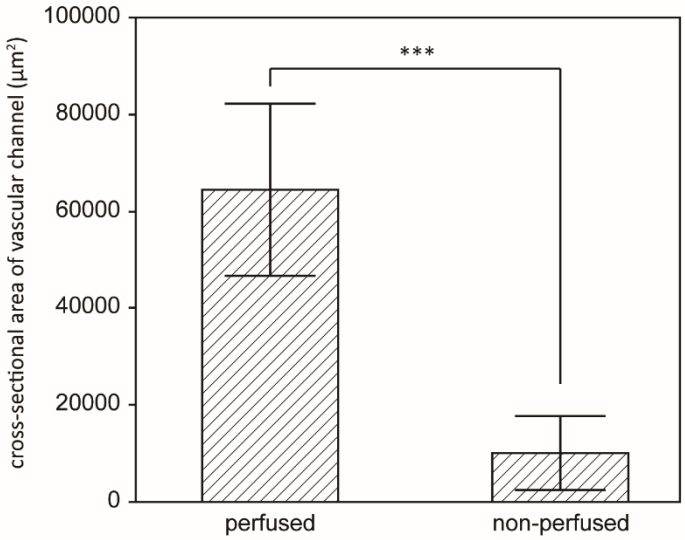

Figure S2. Cross-sectional area of the vascular channels after 7–10 days of perfusion culture. The results are shown as the mean ± standard deviation. ***$p < 0.001$, unpaired Student's *t*-test. $n = 5$ (perfused) and 7 (non-perfused).

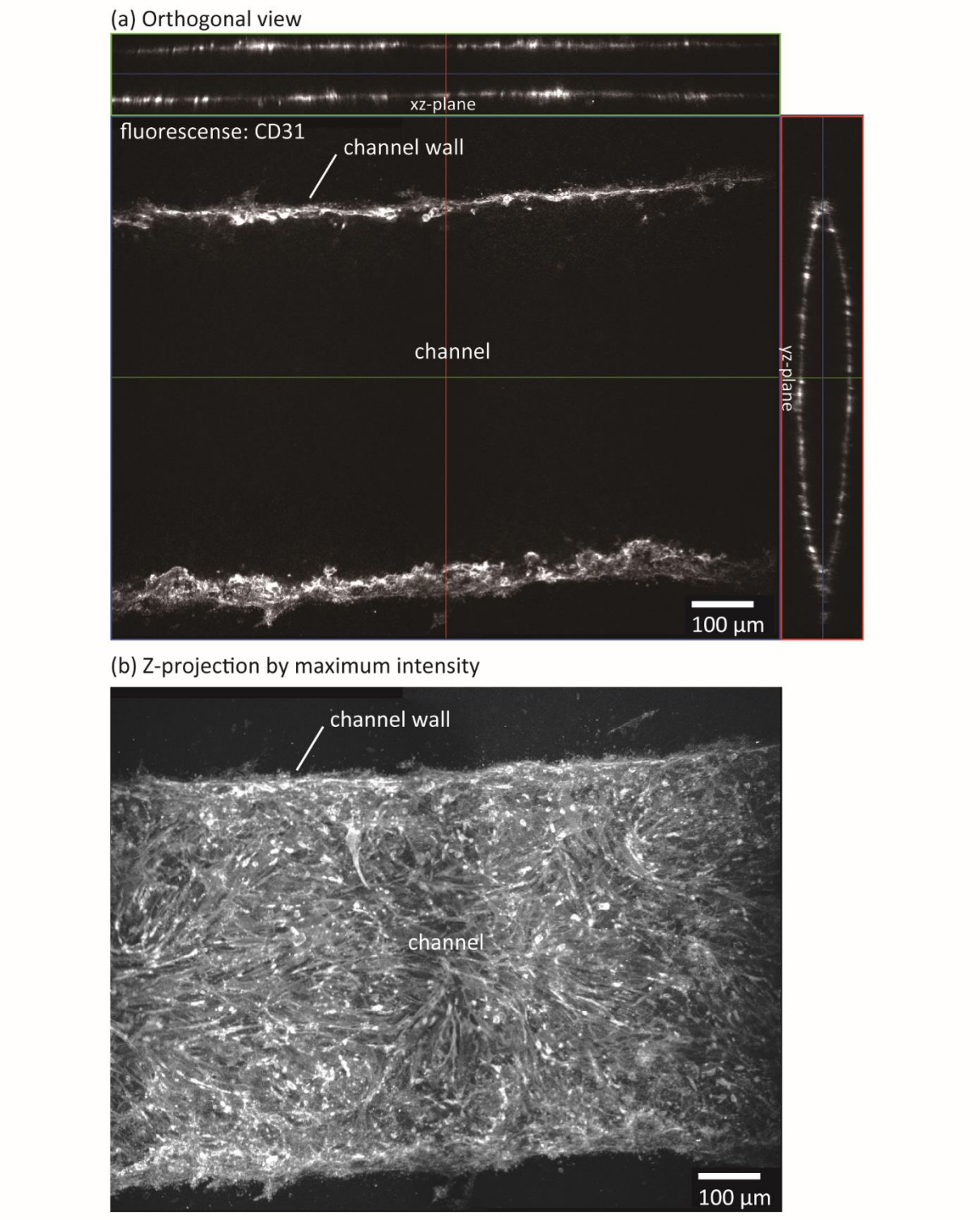

Figure S3. Immunofluorescent image of the vascular channel acquired by two-photon excitation microscopy. (a) Orthogonal view. (b) Z-projected image using maximum intensity.

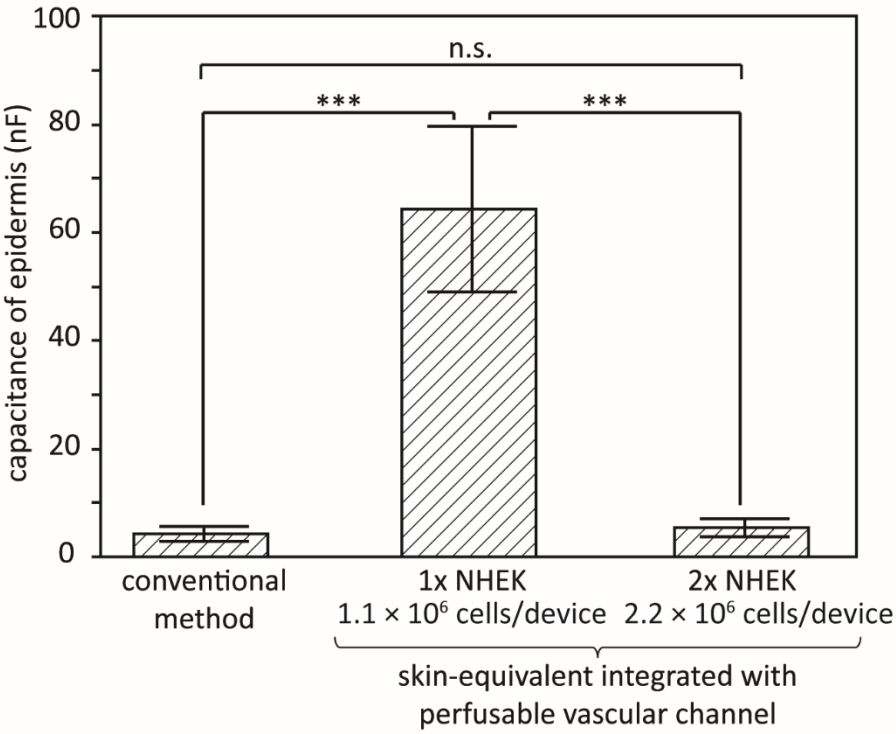

Figure S4. Capacitance of the epidermis layer. The results are shown as the mean ± standard deviation. n.s.: not significant. ***$p < 0.001$, one-way analysis of variance followed by Tukey–Kramer multiple comparison. $n = 6$ (conventional method), 8 (1 × NHEK) and 4 (2 × NHEK).

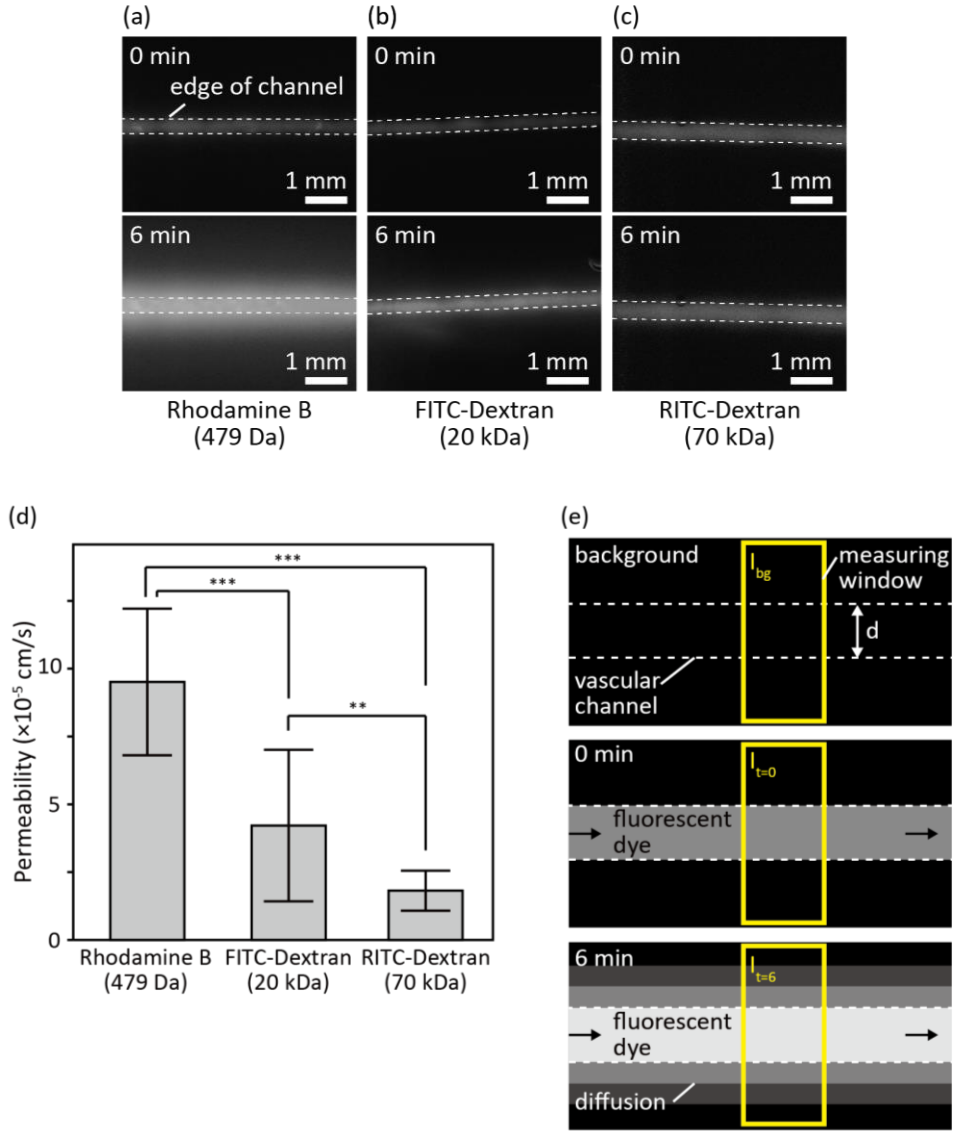

Figure S5. Diffusion of fluorescent molecules from the vascular channels. (a–c) Vascular channels infused with 3 types of molecules: Rhodamine B (479 Da), FITC-Dextran (20 kDa) and RITC-Dextran (70 kDa). (d) Permeability of 3 types of molecules. The results are shown as the mean ± standard deviation. $^{**}p<0.01$, $^{***}p < 0.001$, one-way analysis of variance followed by Tukey–Kramer multiple comparison. n = 17 (8 and 9 measuring windows of 2 devices; Rhodamine B), 23 (7, 7 and 9 measuring windows of 3 devices; FITC-Dextran), and 18 (8 and 10 measuring windows of 2 devices; RITC-Dextran). The number of measuring windows per device was different from each other because measuring windows containing bubbles that might affect the fluorescence measurement were omitted. (e) Schematic of permeability measurement.

Calculation of permeability

Permeability *P* is obtained by the following equation:

$$P = \frac{I_{t=T} - I_{t=0}}{T\,(I_{t=0} - I_{bg})} \cdot \frac{d}{4},$$

where d is the diameter of the channel, I_t is the fluorescent intensity in the measuring window at time t, T is the total elapsed time (6 min in this experiment) and I_{bg} is the background intensity of the measuring window (Fig. S5e).